

Nature of Glycine and Its α -Carbon Radical in Aqueous Solution: A Theoretical Investigation

Geoffrey P. F. Wood,^{†,‡,§} Mark S. Gordon,^{||} Leo Radom,^{†,§} and David M. Smith^{*,⊥}

School of Chemistry and ARC Centre of Excellence for Free Radical Chemistry and Biotechnology, University of Sydney, Sydney, New South Wales 2006, Australia, Department of Chemistry, Iowa State University, Ames, Iowa 50011, and Centre for Computational Solutions in the Life Sciences, Rudjer Boskovic Institute, 10002 Zagreb, Croatia

Received July 23, 2008

Abstract: Quantum chemistry calculations and classical molecular dynamics simulations have been used to examine the equilibria in solution between the neutral and zwitterionic forms of glycine and also of the glycy radical. The established preference (by 30 kJ mol⁻¹) for the zwitterion of glycine was confirmed by both the quantum chemical calculations and the classical molecular dynamics simulations. The best agreement with experiment was derived from thermodynamic integration calculations of explicitly solvated systems, which gives a free energy difference of 36.6 ± 0.6 kJ mol⁻¹. In contrast, for the glycy radical in solution, the neutral form is preferred, with a calculated free energy difference of 54.8 ± 0.6 kJ mol⁻¹. A detailed analysis of the microsolvation environments of each species was carried out by evaluating radial distribution functions and hydrogen bonding patterns. This analysis provides evidence that the change in preference between glycine and glycy radical is due to the inherent gas-phase stability of the neutral α -carbon radical rather than to any significant difference in the solvation behavior of the constituent species.

1. Introduction

Free radicals derived from α -amino acids are known to be important species in many biological processes. For example, the oxygen-centered tyrosyl radical is thought to be involved in photosynthesis as well as in the vital reduction of RNA to DNA.¹ Other peptide radicals have been implicated in a range of areas relevant to human health such as Alzheimer's disease, atherosclerosis, and diabetes as well as aging.^{2–4}

A class of peptide radicals that arises frequently in biological systems are those derived from the homolytic

cleavage of the C α -H bond. Constructive examples of this type may be found in the glycy radical subclass of the radical-SAM superfamily of enzymes, which are important in various metabolic pathways of anaerobic bacteria.⁵ Harmful examples are known to occur frequently as part of the degradation of proteins through fragmentation and rearrangement reactions initiated by reactive oxygen species.² Indeed, mechanisms of this latter type may well be intimately involved in the diseases noted above.

The prevalence of the C α -centered radicals derived from amino acids is thought to be associated with the unusually low C α -H bond dissociation energies (BDEs) of the relevant closed-shell parent species. This is normally attributed to the captodative stabilizing effect of having both electron-withdrawing and electron-donating substituents acting on a single radical center.⁶ While this special stabilizing effect is relatively straightforward in peptide-based C α -radicals, it becomes more complicated in the amino acid building blocks themselves. The complication arises because, in the absence

* Corresponding author e-mail: david.smith@irb.hr.

[†] School of Chemistry, University of Sydney.

[‡] Present address: Laboratory of Computational Chemistry and Biochemistry, Ecole Polytechnique Fédérale de Lausanne, 1015 Lausanne, Switzerland.

[§] ARC Centre of Excellence for Free Radical Chemistry and Biotechnology.

^{||} Iowa State University.

[⊥] Rudjer Boskovic Institute.

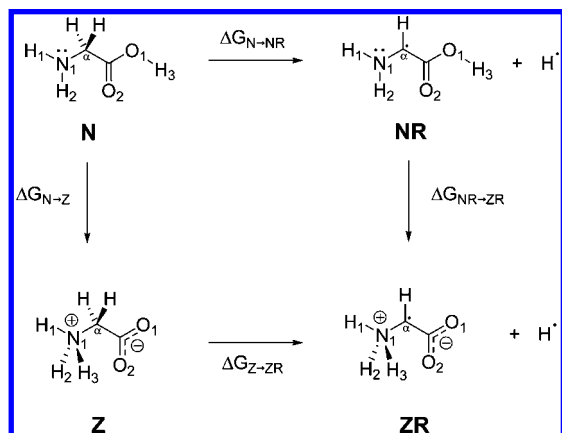


Figure 1. Free energy cycle showing the conversion of neutral glycine (**N**) to zwitterionic glycine (**Z**) (ΔG_{N-Z}) and neutral glycy radical (**NR**) to zwitterionic glycy radical (**ZR**) (ΔG_{NR-ZR}). Alternatively, the cycle may be viewed as showing the C_{α} -H bond dissociations of the closed-shell species **N** (ΔG_{N-NR}) and **Z** (ΔG_{Z-ZR}).

of surrounding peptide bonds, both the closed-shell parent and the C_{α} -radical of an amino acid can potentially exist in either a neutral or a zwitterionic form. In the gas phase, the neutral form is preferred. However, in aqueous solution, the differences between the interaction of the neutral and zwitterionic forms with the solvent can be expected to have a large and possibly even dominating effect on the relative stabilities.

In order to investigate the effect of C_{α} -radical generation on the neutral-zwitterion equilibrium in amino acids, we have chosen to characterize the simplest possible system in which it is present, namely glycine. Using a range of theoretical techniques, we have calculated the relative free energies, both in the gas phase (g) and in aqueous solution (aq), of the neutral and zwitterionic forms of glycine (**N** and **Z**) and the glycy radical (**NR** and **ZR**). Figure 1 shows the four relevant species arranged in the form of a free energy cycle to facilitate both discussion and calculation.⁷

The branch of Figure 1 connecting neutral glycine with its zwitterionic counterpart (ΔG_{N-Z}) has received by far the most attention in the literature.^{8,9} Ab initio studies find that the zwitterion of glycine in the gas phase (**Z**_(g)) is not a local minimum on the potential energy surface but rather collapses to neutral glycine (**N**_(g)).⁹

In contrast to the situation in the gas phase, both the neutral and zwitterionic forms of glycine are stable entities in aqueous solution (**N**_(aq) and **Z**_(aq)), with an experimentally known energy difference in favor of the zwitterion of $\Delta G_{N-Z(aq)} = -30 \text{ kJ mol}^{-1}$.⁸ Because of the fundamental nature of the problem, numerous groups have previously used theory to study the neutral-zwitterion equilibrium of glycine.⁹ However, depending on the level of sophistication employed, the results can show significant variation. Some calculations indicate that the neutral form (**N**_(aq)) is more stable by approximately 5 kJ mol^{-1} , while others favor the zwitterion (**Z**_(aq)) by approximately 50 kJ mol^{-1} .⁹

Although no systematic comparison between the solution-phase energetics of the neutral and zwitterionic forms of the glycy radical has been carried out, Barone and co-workers¹⁰

have undertaken extensive work on their magnetic properties. Their general conclusion, in agreement with indirect experimental evidence,¹¹ is that the neutral form dominates in solution for pH values below 10. In particular, the zwitterion was discounted^{10a,d} because the calculated hyperfine coupling-constant (*hfcc*) values did not agree with the solution-phase experiments but did show agreement with *hfcc* values derived from solid-state glycy radical experiments,¹² in which the radical is known to exist in a zwitterionic form. On the other hand, the calculated *hfcc* values^{10c,d,g} and g-tensors^{10g} for the neutral form agree well with the observed spectroscopic features, provided a sufficiently sophisticated description of the solvent^{10h} is used.

In the present study, we are particularly interested in understanding the details of why the preference for the zwitterionic form of glycine in aqueous solution⁸ changes to a preference for the neutral form in the case of the glycy radical. We approach this question from a thermodynamic point of view, which we believe is complementary to the magnetic approach that has been comprehensively applied to the glycy radical system in recent years.¹⁰

2. Theoretical Methodology

Gas-phase quantum-mechanical energies were obtained with the high-level CBS-QB3 procedure¹³ using Gaussian 03.¹⁴ As mentioned in the Introduction, the zwitterion of glycine in the gas phase (**Z**_(g)) is not a local minimum on the potential energy surface but rather collapses to neutral glycine (**N**_(g)).⁹ In order to investigate the magnitude of $\Delta G_{N-Z(g)}$, we have therefore chosen to use a C_s -symmetry-constrained geometry to approximate the zwitterionic structure (**Z**_(g)). Implicit solvation calculations were performed using a polarizable continuum model (IEF-PCM)¹⁵ with Bondi's all-atom radii and all other parameters appropriate for the solvent water. The geometric contribution to solvation was calculated by re-evaluating the gas-phase CBS-QB3 energies using B3-LYP/6-311G(d,p) geometry optimizations in conjunction with the IEF-PCM methodology. Finally, total free energies in solution and pK_a s were obtained by adding implicit solvation energies derived from IEF-PCM B3-LYP/cc-pVTZ//B3-LYP/6-31+G(d,p) single-point calculations to the re-evaluated CBS-QB3 energies.

Explicit solvation energies were obtained using classical molecular dynamics simulations. Classical valence and van der Waals parameters were assigned to each of the four solutes with the assistance of the antechamber¹⁶ module of the AMBER 8¹⁷ software package. Partial solute charges were obtained by restrained fitting to the electrostatic potentials (RESP)¹⁸ derived from the IEF-PCM B3-LYP/cc-pVTZ//B3-LYP/6-31+G(d,p) calculations mentioned above.¹⁹ Each of the four solutes was placed in a box of 793 TIP3P waters. Following energy minimization of the resultant system in order to remove close contacts, NPT molecular dynamics simulations were run using a 2 fs time step with a coupling constant of 0.2 ps to the constant target temperature of 300 K and a coupling constant of 1.0 ps to the constant target pressure of 1 bar. A 9.0 Å cutoff for nonbonded interactions was used in combination with the particle mesh Ewald procedure for long-range electrostatics,

while bond lengths were constrained using the SHAKE algorithm.²⁰ After an equilibration period of 10 ps, structural data were accumulated over 2 ns for the purpose of radial distribution function (RDF) and H-bond analysis. Following this, the energetic contribution of the solvent to each branch of Figure 1 was obtained by performing the four corresponding alchemical mutations, both in the forward and reverse directions (resulting in eight mutations in total).²¹ The free energy differences associated with these mutations were evaluated using a thermodynamic integration protocol in which only the interactions between the solutes and the solvent were considered. The resulting solvent contributions were then combined with the CBS-QB3 energies to yield the final free energy differences in solution. While the idea of obtaining the solvent contribution to chemical equilibria from classical free energy calculations is not new,²² it has been shown to be an accurate means to access this quantity that still finds widespread applicability in the modern era.²³

In our calculations, the thermodynamic integration was performed using the Gibbs module from the Amber 6 program suite,²⁴ employing electrostatic decoupling. Simulations were run using a 1 fs time step with 20 discrete (λ) windows between each physical state. At each value of λ , 100 ps of equilibration was performed prior to 1 ns of data collection. Coupling constants of 1.0 ps to the target temperature and pressure were employed for these simulations. Further details can be found in the Supporting Information.

3. Results and Discussion

Our approach begins with a gas-phase treatment using the high-level CBS-QB3 procedure.¹³ Application of this methodology yields the gas-phase free energies denoted as $\Delta G_{(g)}$. To supplement these results and arrive at the relevant free energies in aqueous solution ($\Delta G_{(aq)}$), we have used two alternative procedures. The first (implicit) approach involves the polarizable continuum model (PCM) of Tomasi and co-workers.¹⁵ In this approach, the free energy of solvation of each species is calculated and added to the gas-phase free energy. In the second (explicit) approach, suitably parametrized models of the four compounds are placed in a box of 793 TIP3P water molecules and “alchemically” transformed according to the four branches of Figure 1.²¹ The free energies associated with these transformations are then evaluated using thermodynamic integration.²⁵ Due to the fact that free energy is a state function, we may arrange the two differences of differences into an equality

$$\Delta\Delta G = \Delta G_{N \rightarrow NR} - \Delta G_{Z \rightarrow ZR} = \Delta G_{N \rightarrow Z} - \Delta G_{NR \rightarrow ZR} \quad (1)$$

which holds both in the gas phase and in aqueous solution and to which the free energy of the hydrogen atom does not contribute.²¹ Traditionally such a cycle is employed to circumvent the calculation of more “difficult” free energy differences (such as $\Delta G_{N \rightarrow Z} - \Delta G_{NR \rightarrow ZR}$) through their substitution by more “straightforward” evaluations (like $\Delta G_{N \rightarrow NR} - \Delta G_{Z \rightarrow ZR}$). In the current work, however, we have explicitly calculated all four differences.

In the gas phase, the energy difference between the C_s -constrained zwitterionic form of glycine and its neutral

Table 1. Free Energy Differences Relevant to Figure 1 (298 K, kJ mol^{−1})

free energy	CBS-QB3 _(g)	CBS-QB3 _(aq) implicit ^a	CBS-QB3 _(aq) explicit ^b
$\Delta G_{N \rightarrow Z}$	112.0	−50.2	−36.6 ± 0.6 ^c
$\Delta G_{NR \rightarrow ZR}$	200.8	42.3	54.8 ± 0.6 ^c
$\Delta G_{N \rightarrow NR}$	303.9	297.4	300.8 ± 0.2 ^c
$\Delta G_{Z \rightarrow ZR}$	392.8	389.9	400.5 ± 0.1 ^c
$\Delta G_{(N \rightarrow Z - NR \rightarrow ZR)}$	−88.8	−92.5	−91.4 ± 1.2 ^d
$\Delta G_{(N \rightarrow NR - Z \rightarrow ZR)}$	−88.8	−92.5	−99.7 ± 0.3 ^d

^a Solvent effects calculated using the PCM model. ^b Solvent effects calculated using a box of 793 TIP3P water molecules.

^c The tabulated figure represents an average of the results from the simulations run in the forward and reverse directions. The uncertainty reflects half of the difference between these results.

^d The uncertainty is the sum of uncertainties in each branch contributing to the difference.

isomer ($\Delta G_{N \rightarrow Z(g)}$) is 112 kJ mol^{−1} (CBS-QB3, Table 1). On the other hand, using an explicit representation of the solvent yields a value for $\Delta G_{N \rightarrow Z(aq)}$ of $−36.6 \pm 0.6$ kJ mol^{−1} (Table 1), in good agreement with the experimental result ($−30$ kJ mol^{−1}). The implicit approach to solvation also predicts $Z_{(aq)}$ to be more stable than $N_{(aq)}$ (in this case by 50.2 kJ mol^{−1}), but the comparison with experiment is less satisfactory.

While it is not the aim of this study to simply reproduce the equilibrium behavior between the neutral ($N_{(aq)}$) and zwitterionic ($Z_{(aq)}$) forms of glycine, the good agreement with experiment obtained by combining CBS-QB3 gas-phase energies with an explicit classical representation of the solvent, for this equilibrium, is important and encouraging. In particular, this result can be considered as a calibration of the approach, indicating that the chosen methodology can be considered to be reasonably reliable for the closed-shell equilibrium (between $N_{(aq)}$ and $Z_{(aq)}$) and by implication can be expected to be similarly reliable for treating the closely related equilibrium between the neutral and zwitterionic forms of glycol radical ($NR_{(aq)}$ and $ZR_{(aq)}$). Indeed, an approach involving calibration of a methodology with a known result, followed by informed application to a closely related model, has been advocated for some time.²⁶

The CBS-QB3 results predict that the neutral form of the glycol radical $NR_{(g)}$ is significantly more stable (in the gas phase) than the (constrained) zwitterionic form $ZR_{(g)}$, which can be seen by the value of $\Delta G_{NR \rightarrow ZR(g)} = 200.8$ kJ mol^{−1} in Table 1. This large energy difference comes about because, in addition to the contribution arising from charge separation (such as that which dominates $\Delta G_{N \rightarrow Z(g)}$), there is captodative stabilization in the neutral form of the radical ($NR_{(g)}$) that is absent in the zwitterionic counterpart ($ZR_{(g)}$). However, due to the anticipated preferential solvation of the zwitterion ($ZR_{(g)}$), the extent of this difference might be expected to be considerably reduced in aqueous solution, as in the case of glycine itself (N vs Z). Indeed, the value of $\Delta G_{NR \rightarrow ZR(aq)}$ calculated with explicit solvent indicates that the impact of aqueous solvation on this difference is some 146.0 kJ mol^{−1}. However, even this large differential solvation effect is not sufficient to overcome the inherent preference (by 200.8 kJ mol^{−1}) for the neutral radical ($N_{(g)}$), which is predicted to remain the more stable radical species in solution by 54.8

$\pm 0.6 \text{ kJ mol}^{-1}$ (using the explicit model). The implicit solvation model also supports this conclusion but, as was the case for $\Delta G_{\text{N} \rightarrow \text{Z}(\text{aq})}$, this approach probably overstabilizes the zwitterionic form, leading to a prediction of $\Delta G_{\text{NR} \rightarrow \text{ZR}(\text{aq})} = 42.3 \text{ kJ mol}^{-1}$.

Intrigued by the earlier suggestion that a protonated form of the glycy radical ($\text{NH}_2\text{C}(\bullet)\text{HCO}_2\text{H}_2\oplus$) could be necessary to account for the observed magnetic properties in acidic solution,^{10b} we have also calculated the $\text{p}K_{\text{a}}$ values of the two relevant radical-cation species using the implicit approach outlined above. We find that the calculated $\text{p}K_{\text{a}}$ of the species ($\text{NH}_2\text{C}(\bullet)\text{HCO}_2\text{H}_2\oplus$) that would result from protonation of the oxygen atom of the neutral glycy radical is -5.4 . Similarly, the $\text{p}K_{\text{a}}$ of the less stable species, resulting from protonation of the nitrogen ($\oplus\text{NH}_3\text{C}(\bullet)\text{HCO}_2\text{H}$), is calculated to be -4.1 . Both of these values are low, and the true values are likely to be even lower, given that the same methodology overestimates the experimental $\text{p}K_{\text{a}}$ value for the $\oplus\text{NH}_3\text{CH}_2\text{COOH} \rightarrow \oplus\text{NH}_3\text{CH}_2\text{COO}^- + \text{H}^+$ reaction by $0.5 \text{ p}K_{\text{a}}$ units (2.8 as opposed to 2.3 , see Table S3 of the Supporting Information).²⁷ We therefore conclude that it is unlikely for the glycy radical to become protonated, even under strongly acidic conditions. Such a conclusion is compatible with the spectral parameters derived from vibrational-averaging^{10c,d} and molecular dynamics simulations^{10g} presented by Barone and co-workers, which are in turn in good agreement with those measured at a pH of 1.¹¹

Clearly, the presence of a radical center at C_{α} of glycine drastically alters the equilibrium between, and the acidity of, the respective neutral and zwitterionic forms. The extent to which the presence of the radical alters the equilibrium, when compared with the same situation in the closed-shell counterparts, is provided by the quantity $\Delta\Delta G = \Delta G_{\text{N} \rightarrow \text{Z}} - \Delta G_{\text{NR} \rightarrow \text{ZR}}$. As mentioned previously, this is equivalent to the difference in the two bond dissociation energies $\Delta\Delta G = \Delta G_{\text{N} \rightarrow \text{NR}} - \Delta G_{\text{Z} \rightarrow \text{ZR}}$, which in turn can be called a radical stabilization energy.²⁸ Regardless of which branches of the thermodynamic cycle are used, the gas-phase results in Table 1 show that the neutral form of the radical is favored over the zwitterionic form in the gas phase by an additional 88.8 kJ mol^{-1} when compared with the same situation for the closed-shell parent species.

Interestingly, despite the potential for large differences in the solvation energies of the various species in Figure 1, the value of $\Delta\Delta G_{(\text{aq})}$ is not significantly different from $\Delta\Delta G_{(\text{g})}$. In the case of the implicit model, the effect of solvation is predicted to cause $\Delta\Delta G$ to become more negative than the gas-phase value by just 3.7 kJ mol^{-1} . The explicit solvation model also suggests that $\Delta\Delta G_{(\text{aq})}$ is only marginally more negative than $\Delta\Delta G_{(\text{g})}$. In this case, however, the effect is expressed as a range (2.6 – 10.7 kJ mol^{-1}) rather than as a single value.²⁹ In both cases, the minor difference between $\Delta\Delta G_{(\text{g})}$ and $\Delta\Delta G_{(\text{aq})}$ indicates that the reason why there is a qualitative shift accompanying solvation in the equilibrium between the neutral and zwitterionic forms of glycine, but not for the glycy radical, is largely associated with the underlying gas-phase stabilities rather than any drastically different solvation behavior.

Table 2. Charge Values (e) Obtained by the RESP Procedure^a for Neutral Glycine (**N**), the Neutral Glycyl Radical (**NR**), Zwitterionic Glycine (**Z**), and the Zwitterionic Glycyl Radical (**ZR**)

atom	N	NR	Z	ZR
N ₁	−1.071	−0.644	−0.073	−0.136
H ₁	0.398	0.407	0.276	0.321
H ₂	0.398	0.407	0.276	0.321
H ₃	0.520	0.494	0.276	0.321
C _α	0.328	−0.117	0.001	−0.101
H _α	0.040	0.199	0.069	0.152
H _{α'}	0.040		0.069	
C	0.736	0.632	0.758	0.732
O ₁	−0.720	−0.690	−0.826	−0.804
O ₂	−0.670	−0.688	−0.826	−0.804

^a Using electrostatic potentials derived from the IEF-PCM B3-LYP/cc-pVTZ//B3-LYP/6-31+G(d,p) calculations.

The minimal net impact of solvation on $\Delta\Delta G$ shown in Table 1 could be taken to imply that the relative solvation environments of the closed-shell species are quite similar to those of the relevant radical counterparts. In addition to this circumstantial thermodynamic argument, it is possible to probe such phenomena more directly through a detailed structural analysis of the simulations carried out in the present study using explicit water.

Prior to embarking on such a structural analysis however, it is informative to briefly examine the RESP charges obtained for each of the four solutes examined in this study (Table 2). It is through these charge values that the differing electronic distributions, reflected in the differing electrostatic potentials, enter the classical molecular dynamics simulations. Several important factors can be seen by inspection of Table 2. First, the atomic charges for the two zwitterionic species (**Z** and **ZR**) are relatively similar to one another, as demonstrated by the largest difference between them (for C_α) of just 0.1 e . On the other hand, there are more significant differences between the two neutral species (**N** and **NR**). In particular, the charge on the nitrogen is 0.4 e less negative in the radical than in the closed-shell species. This is compensated for by the charge on C_α becoming negative (partially offset by a more positive charge for H_α) and a more negative total charge on the carboxylic acid substituent (from -0.1 to -0.3 e). These results are consistent with the concept of the captodative effect, which sees the radical center receive an increased donation of density from the amino substituent, combined with an increased acceptance by the carboxylic acid substituent.

One means of obtaining an informative overview of the microsolvation of the various species examined in this study is through the inspection of selected radial distribution functions (RDFs). For example, Figure 2 shows the RDFs of water oxygens (O_w) around N₁ (solid lines) and O₂ (dashed lines) of all four species (see Figure 1). The major difference between the neutral (**N** and **NR**) and zwitterionic (**Z** and **ZR**) RDFs is the significantly larger peak heights associated with the latter. This is simply a reflection of the stronger interaction of the more polar species with the aqueous medium, as is also quantitatively evident from the free energy changes shown in Table 1. In accordance with the thermodynamic expectations, the RDFs for the two zwitterionic

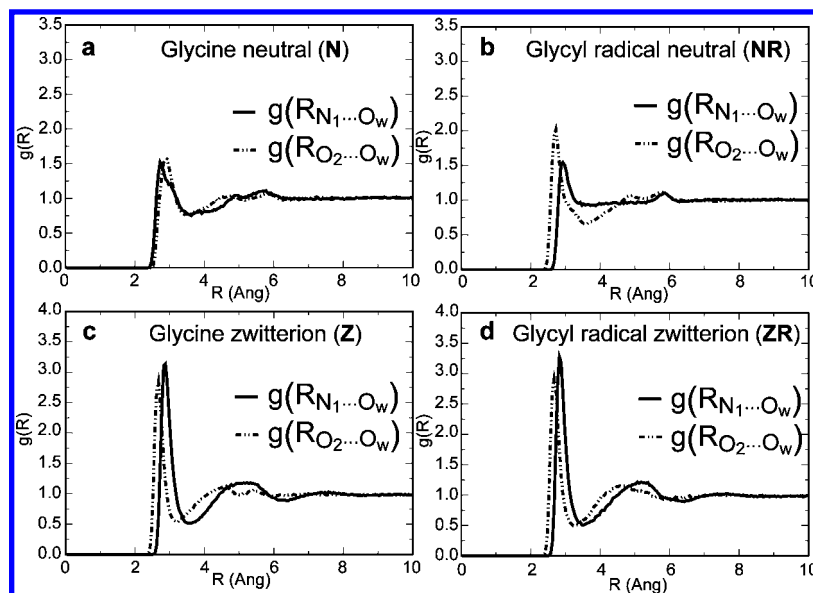


Figure 2. Radial distribution functions ($g(R)$) of water oxygens (O_w) around (a) N_1 (solid lines) and O_2 (dashed lines) of neutral glycine (**N**), (b) N_1 and O_2 of neutral glycyl radical (**NR**), (c) N_1 and O_2 of glycine zwitterion (**Z**), and (d) N_1 and O_2 of glycyl radical zwitterion (**ZR**).

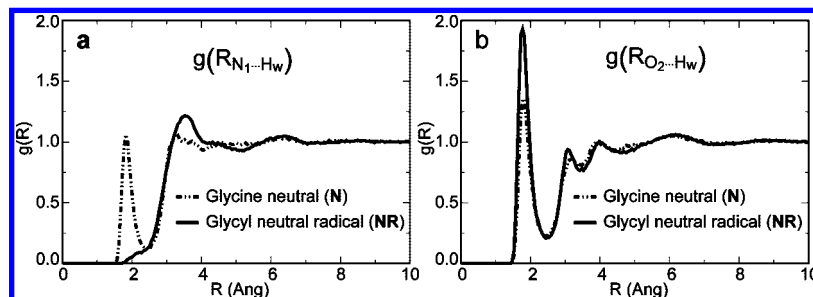


Figure 3. Radial distribution functions of water protons (H_w) around (a) N_1 of neutral glycine (**N**, dashed line) and of neutral glycyl radical (**NR**, solid line) and (b) O_2 of neutral glycine (**N**, dashed line) and of neutral glycyl radical (**NR**, solid line).

systems **Z** and **ZR** can be seen to be very similar to one another (Figure 2c,d). A comparable observation is qualitatively valid for the two neutral systems (**N** and **NR**, Figure 2a,b), although some minor differences are apparent. In particular, the N-atom of the radical (**NR**) appears to be less well solvated than the analogous N-atom in the closed-shell system (**N**). The opposite trend is apparent for the corresponding carbonyl oxygen atom.

Additional information pertaining to the nature of the microsolvation of the N_1 and O_2 atoms of neutral glycine (**N**) and its C_α -derived radical (**NR**) is provided by the RDFs of the water protons (H_w) surrounding these atoms. For example, the RDFs of solvent protons surrounding the nitrogen atom shown in Figure 3a are markedly different for species **N** and **NR**. In particular, the absence of the peak centered at $\sim 2 \text{ \AA}$ in the solid curve gives a strong indication that the lone pair on the N-atom acts as a substantially weaker hydrogen-bond acceptor in the C_α -radical (**NR**) than in neutral glycine (**N**) itself. Such behavior can be rationalized in terms of the enhanced (captodative) delocalization in the glycyl radical, for example by making the nitrogen lone pair less accessible for H-bonding. Insofar as hydrogen-bonding tendencies are related to proton affinity,³⁰ this result can also be connected to the reduced basicity at the nitrogen atom in the glycyl radical. The loss of H-bond-accepting ability at

Table 3. Average Number of Hydrogen Bonds for the Duration of the Simulations between Water and Various Sites on Neutral Glycine (**N**), the Neutral Glycyl Radical (**NR**), Zwitterionic Glycine (**Z**), and the Zwitterionic Glycyl Radical (**ZR**)

site	N _(aq)	NR _(aq)	site	Z _(aq)	ZR _(aq)
N_1-H_1	0.9	1.0	N_1-H_1	1.1	1.1
N_1-H_2	0.9	1.0	N_1-H_2	1.1	1.1
N_1	1.4	0.3	N_1-H_3	1.1	1.1
O_1-H_3	1.0	1.0	O_1	3.5	3.3
O_2	2.0	2.5	O_2	3.5	3.7

this atom appears to be partially compensated for by a concomitant increase in the H-bond-accepting ability at the carbonyl oxygen of the same species (**NR**). This is manifested in the enhanced peak height associated with the solid curve in Figure 3b.

In addition to the RDF analysis presented above, we have also probed the microsolvation of all four species by monitoring H-bonds throughout the relevant trajectories, where an H-bond $X-H\cdots Y$ is defined to exist if the $X\cdots Y$ length is less than 3.5 \AA and the angle defined by the three centers comprising the bond is between 120.0° and 180.0° . The results of this analysis, which are shown in Table 3, serve to provide quantitative confirmation of the conclusions

suggested by the RDFs. Specifically, the effect of H-atom loss on the solvation of glycine zwitterion is rather minimal (recall the similarity between parts c and d of Figure 2). The average H-bonding behavior of the NH_3^+ group can be seen to be virtually identical for the closed-shell (**Z**) and open-shell (**ZR**) species. The carboxylate oxygens exhibit a minor loss of mutual equivalence in the radical (**ZR**), but the average H-bond-accepting capacity of the CO_2^- group appears to be unaffected by C_α -radical formation.

The H-bond-donating abilities of the $\text{N}_1\text{--H}$ and $\text{O}_1\text{--H}_3$ groups of the neutral systems also remain virtually unaltered in response to radical generation. On the other hand, the degree of H-bond acceptance by both N_1 and O_2 does seem to differ significantly between the closed- and open-shell neutral systems. In quantitative support of the graphical interpretation presented in Figure 3, the average number of H-bonds accepted by N_1 in the neutral radical (**NR**) (0.3) is reduced by 1.1 (from 1.4) with respect to the closed-shell parent (**N**). At the same time, the H-bond-accepting capacity of O_2 (2.5) is enhanced in the radical (**NR**) by 25% compared with that observed (2.0) for the closed-shell species (**N**). Again, the result is readily rationalized in terms of the captodative delocalization in the glycyl radical.

4. Concluding Remarks

In summary, we have used a variety of theoretical means to investigate the comparative equilibria between the neutral and zwitterionic forms of glycine and its C_α -radical. Our calculations show that an explicit classical representation of the solvent is able to satisfactorily reproduce the known magnitude of the free energy preference for zwitterionic glycine in aqueous solution. An analogous application of the same methodology to the glycyl radical shows that, in contrast to the closed-shell parent system, the neutral form is preferred in solution by approximately 55 kJ mol^{-1} . Examination of the components of this difference reveals that this preference can be almost entirely attributed to the captodative stabilization of the neutral radical in the gas-phase reference state. In other words, even though the zwitterionic radical is significantly better solvated than the neutral radical, the extent of this interaction is not sufficient to overcome the underlying preferential gas-phase stabilization in the neutral glycyl radical. In a related finding, our calculations indicate that it is very unlikely for the neutral glycyl radical to become protonated, even at very low pH values.

A convenient quantitative measure of the relevant differential stabilization is provided by the quantity denoted in the present study as $\Delta\Delta G$, the difference between the zwitterionic and neutral energies for glycine on the one hand and the glycyl radical on the other. Our calculations predict that $\Delta\Delta G$ adopts a value in the gas phase of 88.8 kJ mol^{-1} . Despite the potential for solvation to have a substantial effect on this quantity, our best prediction for the value of $\Delta\Delta G_{\text{(aq)}}$ lies between 90 and 100 kJ mol^{-1} , indicating that the impact of the aqueous medium in this case is, in actual fact, quite minor. Analysis of the microsolvation patterns of the four species investigated in the present study supports this conclusion. While large differences are found when col-

lectively comparing the neutral (**N** and **NR**) with the zwitterionic (**Z** and **ZR**) systems, each open-shell and closed-shell pair is found to exhibit relatively similar general solvation patterns. An important difference arises for the neutral pair (**N** and **NR**), for which the N-atom of the C_α radical (**NR**) is found to exhibit a markedly reduced propensity for H-bond acceptance (compared with **N**), whereas the carbonyl oxygen of the radical experiences an apparently compensatory effect. This phenomenon again appears to be a consequence of the simultaneous and synergistic action of π -electron-donating (NH_2) and π -electron-accepting (CO_2H) substituents adjacent to a radical center.

Acknowledgment. We gratefully acknowledge the award (to L.R.) of an Australian Research Council Discovery grant, funding (to L.R. and G.P.F.W.) through the ARC Centre of Excellence for Free Radical Chemistry and Biotechnology, and generous allocations of computer time from the Australian Partnership for Advanced Computing (APAC) and the Australian Centre for Advanced Computing and Communications (AC3). We also acknowledge support (for M.S.G) from the U.S. Air Force Office of Scientific Research and the Australia Fulbright Association. Finally, the support (of D.M.S) by the Croatian Ministry of Science (project 098-0982933-2937) and the E.C. (FP6 contract 043749) is gratefully acknowledged.

Supporting Information Available: Gaussian archive entries (Table S1), extracts from Amber prep files (Table S2), details of pK_a evaluations (Table S3), and details of the convergence of the RDFs and thermodynamic integration calculations (Table S4). This material is available free of charge via the Internet at <http://pubs.acs.org>.

References

- (1) Stubbe, J.; van der Donk, W. *Chem. Rev.* **1998**, *98*, 705, and references therein.
- (2) Davies, M. J.; Dean, R. T. *Radical-Mediated Protein Oxidation: from Chemistry to Medicine*; Oxford University Press: Oxford; New York, 1997; pp 203–237, and references therein.
- (3) Dean, R. T.; Fu, S.; Stocker, R.; Davies, M. J. *Biochem. J.* **1997**, *324*, 1.
- (4) (a) Rauk, A.; Armstrong, D. A.; Fairlie, D. P. *J. Am. Chem. Soc.* **2000**, *122*, 9761. (b) Rauk, A. *Can. Chem. News* **2001**, *53*, 20. (c) Brunelle, P.; Rauk, A. *J. Alzheimer's Dis.* **2002**, *4*, 283.
- (5) (a) Frey, P. A.; Magnusson, O. T. *Chem. Rev.* **2003**, *103*, 2129. (b) Wang, S. C.; Frey, P. A. *Trends Biochem. Sci.* **2007**, *32*, 101.
- (6) (a) Viehe, H. G.; Janouesk, Z.; Merenyi, R.; Stella, L. *Acc. Chem. Res.* **1985**, *18*, 148. (b) Easton, C. J. *Chem. Rev.* **1997**, *97*, 53. (c) Rauk, A.; Yu, D.; Taylor, J.; Shustov, G. V.; Block, D. A.; Armstrong, D. A. *Biochemistry* **1999**, *38*, 9089. (d) Wood, G. P. F.; Moran, D.; Jacob, R.; Radom, L. *J. Phys. Chem. A* **2005**, *109*, 6318.
- (7) Throughout this paper, the quantity $\Delta G_{\text{m} \rightarrow \text{n}}$ refers to the free energy difference $G_{\text{n}} - G_{\text{m}}$.
- (8) Wada, G.; Tamura, E.; Okina, M.; Nakamura, M. *Bull. Chem. Soc. Jpn.* **1982**, *55*, 3064.

- (9) See for example: (a) Gaffney, J. S.; Pierce, R. C.; Friedman, L. *J. Am. Chem. Soc.* **1977**, *99*, 4293. (b) Clementi, E.; Cavallone, F.; Scordamaglia, R. *J. Am. Chem. Soc.* **1977**, *99*, 5531. (c) Tse, Y. C.; Newton, M. D.; Vishveshwara, S.; Pople, J. A. *J. Am. Chem. Soc.* **1978**, *100*, 4329. (d) Jensen, J. H.; Gordon, M. S. *J. Am. Chem. Soc.* **1995**, *117*, 8159. (e) Nagaoka, M.; Okuyama-Yoshida, N.; Yamabe, T. *J. Phys. Chem. A* **1998**, *102*, 8202. (f) Bandyopadhyay, P.; Gordon, M. S. *J. Chem. Phys.* **2000**, *113*, 1104. (g) Shoeib, T.; Ruggiero, G. D.; Siu, M. K. W.; Hopkinson, A. C.; Williams, I. H. *J. Chem. Phys.* **2002**, *117*, 2762. (h) Leung, K.; Rempe, S. B. *J. Chem. Phys.* **2005**, *122*, 184506. (i) Aikens, C. M.; Gordon, M. S. *J. Am. Chem. Soc.* **2006**, *128*, 12835. (j) Chang, J.; Lenhoff, A. M.; Sandler, S. I. *J. Phys. Chem. B* **2007**, *111*, 2098. (k) Bachrach, S. M. *J. Phys. Chem. A* **2008**, *112*, 3722.
- (10) (a) Barone, V.; Adamo, C.; Grand, A.; Subra, R. *Chem. Phys. Lett.* **1995**, *242*, 351. (b) Barone, V.; Adamo, C.; Grand, A.; Jolibois, F.; Brunel, Y.; Subra, R. *J. Am. Chem. Soc.* **1995**, *117*, 12618. (c) Rega, N.; Cossi, M.; Barone, V. *J. Am. Chem. Soc.* **1997**, *119*, 12962. (d) Rega, N.; Cossi, M.; Barone, V. *J. Am. Chem. Soc.* **1998**, *120*, 5723. (e) Ciofini, I.; Adamo, C.; Barone, V. *J. Chem. Phys.* **2004**, *121*, 6710. (f) Brancato, G.; Barone, V.; Rega, N. *Theor. Chem. Acc.* **2007**, *117*, 1001. (g) Brancato, G.; Rega, N.; Barone, V. *J. Am. Chem. Soc.* **2007**, *129*, 15380. (h) Brancato, G.; Rega, N.; Barone, V. *J. Chem. Phys.* **2008**, *128*, 144501.
- (11) (a) Paul, H.; Fischer, H. *Helv. Chim. Acta* **1971**, *54*, 485. (b) Neta, P.; Fessenden, R. W. *J. Phys. Chem.* **1971**, *75*, 738.
- (12) Nunone, K.; Muto, H.; Torivama, K.; Iwasaki, M. *J. Chem. Phys.* **1976**, *65*, 3805.
- (13) (a) Montgomery, J. A., Jr.; Frisch, M. J.; Ochterski, J. W.; Petersson, G. A. *J. Chem. Phys.* **1999**, *110*, 2822. (b) Montgomery, J. A., Jr.; Frisch, M. J.; Ochterski, J. W.; Petersson, G. A. *J. Chem. Phys.* **2000**, *112*, 6532.
- (14) Frisch, M. J.; Trucks, G. W.; Schlegel, H. B.; Scuseria, G. E.; Robb, M. A.; Cheeseman, J. R.; Montgomery, J. A., Jr.; Vreven, T.; Kudin, K. N.; Burant, J. C.; Millam, J. M.; Iyengar, S. S.; Tomasi, J.; Barone, V.; Mennucci, B.; Cossi, M.; Scalmani, G.; Rega, N.; Petersson, G. A.; Nakatsuji, H.; Hada, M.; Ehara, M.; Toyota, K.; Fukuda, R.; Hasegawa, J.; Ishida, M.; Nakajima, T.; Honda, Y.; Kitao, O.; Nakai, H.; Klene, M.; Li, X.; Knox, J. E.; Hratchian, H. P.; Cross, J. B.; Bakken, V.; Adamo, C.; Jaramillo, J.; Gomperts, R.; Stratmann, R. E.; Yazyev, O.; Austin, A. J.; Cammi, R.; Pomelli, C.; Ochterski, J. W.; Ayala, P. Y.; Morokuma, K.; Voth, G. A.; Salvador, P.; Dannenberg, J. J.; Zakrzewski, V. G.; Dapprich, S.; Daniels, A. D.; Strain, M. C.; Farkas, O.; Malick, D. K.; Rabuck, A. D.; Raghavachari, K.; Foresman, J. B.; Ortiz, J. V.; Cui, Q.; Baboul, A. G.; Clifford, S.; Cioslowski, J.; Stefanov, B. B.; Liu, G.; Liashenko, A.; Piskorz, P.; Komaromi, I.; Martin, R. L.; Fox, D. J.; Keith, T.; Al-Laham, M. A.; Peng, C. Y.; Nanayakkara, A.; Challacombe, M.; Gill, P. M. W.; Johnson, B.; Chen, W.; Wong, M. W.; Gonzalez, C.; Pople, J. A. *GAUSSIAN 03, Revision C.02*; Gaussian, Inc.: Wallingford, CT, 2004.
- (15) (a) Munnuci, B.; Tomasi, J. *J. Chem. Phys.* **1997**, *106*, 5151. (b) Cancès, M. T.; Munnuci, B.; Tomasi, J. *J. Chem. Phys.* **1997**, *107*, 3032. (c) Cossi, M.; Munnuci, B.; Tomasi, J. *Chem. Phys. Lett.* **1998**, *286*, 253.
- (16) Wang, J.; Wang, W.; Kollman, P. A.; Case, D. A. *J. Mol. Graphics Modell.* **2006**, *25*, 247–260.
- (17) Case, D. A.; Darden, T. A.; Cheatham, T. E., III; Simmerling, C. L.; Wang, J.; Duke, R. E.; Luo, R.; Merz, K. M.; Wang, B.; Pearlman, D. A.; Crowley, M.; Brozell, S.; Tsui, V.; Gohlke, H.; Mongan, J.; Hornak, V.; Cui, G.; Beroza, P.; Schafmeister, C.; Caldwell, J. W.; Ross, W. S.; Kollman, P. A. *AMBER 8*; University of California: San Francisco, CA, 2004.
- (18) Bayly, C. I.; Cieplak, P.; Cornell, W. D.; Kollman, P. A. *J. Phys. Chem.* **1993**, *97*, 10269.
- (19) This procedure is similar to that employed in the following: Duan, Y.; Wu, C.; Chowdhury, S.; Lee, M. C.; Xiong, G.; Zhang, W.; Yang, R.; Cieplak, P.; Luo, R.; Lee, T.; Caldwell, J. W.; Wang, J.; Kollman, P. A. *J. Comput. Chem.* **2003**, *24*, 1999.
- (20) Ryckaert, J. P.; Cicciotti, G.; Berendsen, H. J. C. *J. Comput. Phys.* **1977**, *23*, 2272.
- (21) The simulations of the explicit solvation contributions to $\Delta G_{N \rightarrow NR(aq)}$ and $\Delta G_{Z \rightarrow ZR(aq)}$ involved the direct mutation of **N** (or **Z**) to **NR** (or **ZR**), and no attempt was made to simulate the bare hydrogen atom in a box of water. For the purpose of reporting BDEs, the solvation free energy used for the H-atom (5.4 kJ mol^{-1}) was taken from an implicit PCM calculation. It is important to note that this quantity cancels entirely from $\Delta \Delta G_{(N \rightarrow NR - Z \rightarrow ZR)}$ (Table 1) as well as from $\Delta G_{NR \rightarrow ZR(aq)}$.
- (22) Jorgensen, W. L.; Ravimohan, C. *J. Chem. Phys.* **1985**, *83*, 3050.
- (23) See, for example Jorgensen, W. L.; Thomas, L. L. *J. Chem. Theory Comput.* **2008**, *4*, 869.
- (24) Case, D. A.; Pearlman, D. A.; Caldwell, J. W.; Cheatham, T. E., III; Ross, W. S.; Simmerling, C. L.; Darden, T. A.; Merz, K. M.; Stanton, R. V.; Cheng, A. L.; Vincent, J. J.; Crowley, M.; Tsui, V.; Radmer, R. J.; Duan, J.; Pitera, J.; Massova, I. G.; Seibel, L.; Singh, U. C.; Weiner, P. K.; Kollman, P. A. *AMBER 6*; University of California: San Francisco, CA, 1999.
- (25) Straatsma, T. P.; McCammon, J. A. *J. Chem. Phys.* **1991**, *95*, 1175.
- (26) (a) Pople, J. A. In *Theoretical Models for Chemistry, Proceedings of the Summer Research Conference on Theoretical Chemistry, Energy Structure and Reactivity*; Smith, D. W., Ed.; John Wiley & Sons: New York, 1973; pp 51–61. (b) See also Pople, J. A. *J. Chem. Phys.* **1965**, *48*, 229.
- (27) See for example: Nelson, D. L.; Cox, M. M. *Lehninger Principles of Biochemistry*, 5th ed.; W. H. Freeman: New York, 2008; p 73.
- (28) (a) See for example Henry, D. J.; Parkinson, C. J.; Mayer, P. M.; Radom, L. *J. Phys. Chem. A* **2001**, *105*, 6750, and references therein. (b) For a recent comprehensive review on radical stability, see Zipse, H. *Top. Curr. Chem.* **2006**, *263*, 163.
- (29) The range in values comes about because of inadequacies in the numerical integration scheme.
- (30) See for example Chan, B.; Del Bene, J. E.; Elguero, J.; Radom, L. *J. Phys. Chem. A* **2005**, *109*, 550.

CT8002942